Research Article | Vol. 11, No. 9 / 1 September 2020 / Biomedical Optics Express 5341
Biomedical Optics EXPRESS

Irradiation effect of a submillimeter wave from 420 GHz gyrotron on amyloid peptides in vitro

TAKAYASU KAWASAKI,[1,*] YUUSUKE YAMAGUCHI,[2] TOMOMI UEDA,[3] YUYA ISHIKAWA,[2] TOYONARI YAJI,[4] TOSHIAKI OHTA,[4] KOICHI TSUKIYAMA,[1] TOSHITAKA IDEHARA,[2] MASATOSHI SAIKI,[3] AND MASAHIKO TANI[2]

[1]*IR-FEL Research Center, Research Institute for Science and Technology, Organization for Research Advancement, Tokyo University of Science, 2641 Yamazaki, Noda, Chiba 278-8510, Japan*
[2]*Research Center for Development of Far-Infrared Region, University of Fukui, 3-9-1 Bunkyo, Fukui, Fukui 910-8507, Japan*
[3]*Department of Applied Chemistry, Faculty of Engineering, Sanyo-Onoda City University, 1-1-1 Daigakudori, Sanyo-Onoda, Yamaguchi 756-0884, Japan*
[4]*SR Center, Research Organization of Science and Technology, Ritsumeikan University, 1-1-1 Noji-Higasi, Kusatsu, Shiga 525-8577, Japan*
[*]*kawasaki@rs.tus.ac.jp*

Abstract: On using the far-infrared radiation system, whether the irradiation effect is thermal or non-thermal is controversial. We irradiated amyloid peptides that are causal factors for amyloidosis by using a submillimeter wave from 420 GHz gyrotron. Fluorescence reagent assay, optical and electron microscopies, and synchrotron-radiation infrared microscopy showed that the irradiation increased the fibrous conformation of peptides at room temperature for 30 min. The temperature increase on the sample was only below 5 K, and a simple heating up to 318 K hardly induced the fibril formation. Therefore, the amyloid aggregation was driven by the far-infrared radiation with little thermal effect.

1. Introduction

In recent years, physical engineering techniques using far-infrared electromagnetic waves have been gained interest in the chemical and biomedical research fields. Typically, microwave heating is used for organic chemical reactions such as solid-phase peptide synthesis and metal-based nanoparticle preparations [1,2]. In addition, far-infrared radiation and lasers are often used for biological and medical studies using cell line systems for the development of phototherapies and photo-diagnostics of cancer cells [3–5]. The oscillation frequency of microwaves is usually low gigahertz (GHz), and the power reaches ~10 kW. These physical features can cause remarkable structural changes to target biomolecules, and the high permeability of biological tissues to far-infrared light is frequently effective for *in vivo* imaging [6]. Thus, target substances are often heated by the radiation. However, whether the radiation effect is thermal or non-thermal is a question of some controversy.

The self-assembly of amyloids plays various roles in the expression of biological functions [7,8]. It is closely associated with the development of serious amyloidosis such as Alzheimer's disease. The aggregation reaction of amyloid β protein proceeds over several days under physiological conditions, after which the fibrous aggregates are deposited into the various tissues. Protecting against neurodegenerative diseases is urgently required for our aging society. However, some species of amyloids work as functional regulators of gene expression in microorganisms [9]. Further, functional amyloids are employed as extracellular matrix for cell adhesion and colony formation as shown in biofilms. Additionally, the β-sheet stacked conformation is thermodynamically stable under physiological conditions and the rigid fiber format can be used

#395218 https://doi.org/10.1364/BOE.395218
Journal © 2020 Received 22 Apr 2020; revised 7 Aug 2020; accepted 7 Aug 2020; published 31 Aug 2020

Biomedical Optics EXPRESS

as a reliable scaffold for biocompatible materials [10,11]. Therefore, structural control of the self-assembly process will potentially lead to the processing of the solid fiber-like biomaterials and the regulation of biochemical reactions associated with amyloid fibrils.

In this work, we applied a far-infrared ray generated by a gyrotron to irradiate amyloid peptides *in vitro*. A gyrotron is a type of electron vacuum tube which can emit submillimeter waves having dozens to kilo W powers in the GHz to terahertz (THz) frequency range and is frequently employed for nuclear magnetic resonance systems [12]. Although the high radiation energy emitted by the gyrotron is expected to affect various biological and chemical substances, few biomedical studies on the topic have been reported [13,14]. We employed a 420 GHz gyrotron that can generate an electromagnetic wave of 720 μm and targeted one functional amyloid peptide from *Saccharomyces cerevisiae* and three disease-related amyloid peptides from human tissues. Those peptides have been thoroughly investigated in the biochemical and medical fields: 1) Sup35 seven-residue fragment GNNQQNY, 2) amyloid β ($A\beta_{1-40}$), 3) serum amyloid A (SAA), and 4) calcitonin penta-peptide DFNKF.

GNNQQNY is part of a sequence of a yeast prion-like protein that is associated with gene regulation in the bacteria [15,16]. $A\beta_{1-40}$ is a causal factor for the onset of Alzheimer's disease [17,18]. SAA is associated with systemic amyloidosis causing rheumatoid arthritis [19,20]. Among the entire sequence of SAA, the fragment 1-27 tends to fibrillate spontaneously whereas the fragment 51-80 and other C-terminal sequences do not form fibrils, as determined by co-author Saiki (unpublished). DFNKF is part of a sequence of a thyroid hormone that is associated with medullary carcinoma [21,22].

The structural changes to these synthetic peptides following far-infrared radiation were analyzed by using fibril-binding reagents, optical and electron microscopies, and synchrotron-radiation infrared microscopy coupled with protein secondary conformation analysis.

2. Materials and methods

2.1. Materials

Dimethyl sulfoxide (DMSO), phosphate buffered saline (PBS; 10 mM, pH 7.2–7.4 at 25 °C), and sodium chloride were purchased from Wako Pure Chemical Industries (Osaka, Japan). Congo Red and 1,1,1,3,3,3-hexafluoro-2-propanol (HFP) were from Sigma-Aldrich (St. Louis, MO). Thioflavin T was purchased from NACALAI TESQUE, INC. (Kyoto). $A\beta_{1-40}$ (90% purity) was from Peptide Institute Inc. (Osaka, Japan). Serum amyloid A (SAA) amyloidogenic fragment (1-27) and non-amyloidogenic fragment (51-80) were synthesized by solid-phase peptide synthesis using an F-moc strategy. GNNQQNY (85% purity) and DFNKF (94.5% purity) were purchased from PH Japan Co., Ltd. (Hiroshima).

2.2. Sample preparation

GNNQQNY was dissolved in 20% acetic acid (pH 3–4) and stored at –30 °C (concentration: 10 mg/mL). The solution (10 μL) was put on a gold-coated glass slide just before the far-infrared irradiation. In order to initiate fibrillation without irradiation, the stock solution (100 μL) was incubated at 37 °C for 20 h. The SAA fragment was dissolved at a concentration of 15 μM in 50 mM sodium acetate buffer (pH 4) in the presence of heparin (41 mg/mL). The solution (10 μL) was put on the metal-coated base just before the irradiation. $A\beta_{1-40}$ was dissolved in 0.27 mL of HFP and then dried *in vacuo*. The resulting pellet was re-dissolved in DMSO (1.0 mM) as a stock solution. Just before the irradiation experiment, the solution was diluted with PBS to 0.1 mM, and the solution was put on the metal surface for the irradiation. DFNKF was dissolved at a concentration of 100 mg/mL in DMSO as a stock solution, then diluted to 10 mg/mL using a buffer (10 mM of tris-base and 20 mM of NaCl, pH7.5) right before the irradiation experiment.

Biomedical Optics EXPRESS

The solution (10 μL) was put on the metal slide base for infrared microscopy analysis or a glass slide base for Congo-red observation.

2.3. Irradiation system

We used the Gyrotron FU CW GVIB far-infrared radiation system, which can expose samples to a 420 GHz wave with a maximum power of 20 W [23]. The radiation wavelength was 720 μm, and the pulse duration was 1 ms at 5 Hz oscillation. The temperature increase of the sample during the irradiation was monitored using a Testo 875 thermography camera (Testo). The amyloid sample in aqueous solution (10 μL) was put on the slide base and was irradiated with the far-infrared ray at room temperature (ca. 25 °C).

2.4. Optical microscope observation

The SAA fragment in the buffer solution was added on a gold-coated slide base. After drying under atmosphere, the sample surface was observed using an Area PIII-FX (SK-Electronics Co., LTD., Kyoto, Japan) microscope with a high-magnification object lens (×200–2000). Images were obtained using a 12 million-pixel CCD camera under the halogen lamp. Images of the sample surface were obtained using Perfect Viewer 7 imaging software (SK-Electronics Co., LTD., Kyoto, Japan).

2.5. Synchrotron-radiation infrared microscopy (SR-IRM)

SR-IRM can enhance spatial resolution with a high signal-to-noise (S/N) ratio compared to the use of a thermal radiation beam. Additionally, the SR-IRM spectrum is sensitive to the secondary structural changes such as α-helix, β-sheet, turn and non-ordered structures of proteins. SR-IRM analysis was performed using the IR micro-spectroscopy beamline (SRMS, BL-15) at the SR Center of Ritsumeikan University [24]. In the optical system, one toroidal mirror and two plane mirrors were used in the storage ring chamber to collect the SR photons in the mid- and far-infrared regions. The beamline was equipped with a Nicolet 6700 FT-IR spectroscope and a Continuum XL infrared microscope (Thermo Fisher Scientific). Measurements were taken in reflection mode with a 32 x Cassegrain lens and a 20 μm x 20 μm aperture and the spectra were recorded in the mid-IR range of 700–4000 cm^{-1} at a resolution of 4 cm^{-1} with 64 scans. Spectra smoothing and normalization was performed using Spectra Manager software ver2 (Jasco International, Tokyo, Japan). Protein secondary structure contents were calculated by de-convolution of the amide I band (1600–1700cm^{-1}) using the attached protein analysis software, IR-SSE (JASCO).

2.6. Thioflavin T (ThT) assay

The amyloid sample was dissolved in PBS (20 μL), and the solution was added to the ThT reagent solution (25 μM). Total volume was set to 100 μL using water. The mixture was incubated for 10 min at room temperature, and the fluorescence intensity was measured at 492 nm using an excitation wavelength of 450 nm on a microplate reader Varioskan Flash (Thermo Fisher Scientific). The measurement was performed several times, and the data were statistically treated.

2.7. Scanning-electron microscopy (SEM)

SEM imaging was performed using an FE-SEM Supra40 scanning electron microscope (Carl Zeiss). After irradiation by the gyrotron as described above, the slide base was fixed on a sample holder by using conductive copper tape. The surface of the sample was observed using an acceleration voltage of 5.0 kV.

Biomedical Optics EXPRESS

2.8. Congo-red staining

The reagent solution (0.2 mM in PBS, 10 μL) was added to the amyloid sample on a glass slide. After drying, the sample surface was observed by a polarized light microscope (MVX 10, Olympus, Tokyo, Japan).

3. Results

The radiation beam was directed from the beam port of the gyrotron to the peptide sample via reflective mirrors (Fig. 1). The sample temperature was ~27 °C and 30 °C during irradiation at 10 W and 20 W, respectively, as shown in the thermography camera images (Fig. 1(b)). Thus, the temperature increased by less than 5 K during the far-infrared radiation. The water in the sample was spontaneously vapored within 30 min during the irradiation.

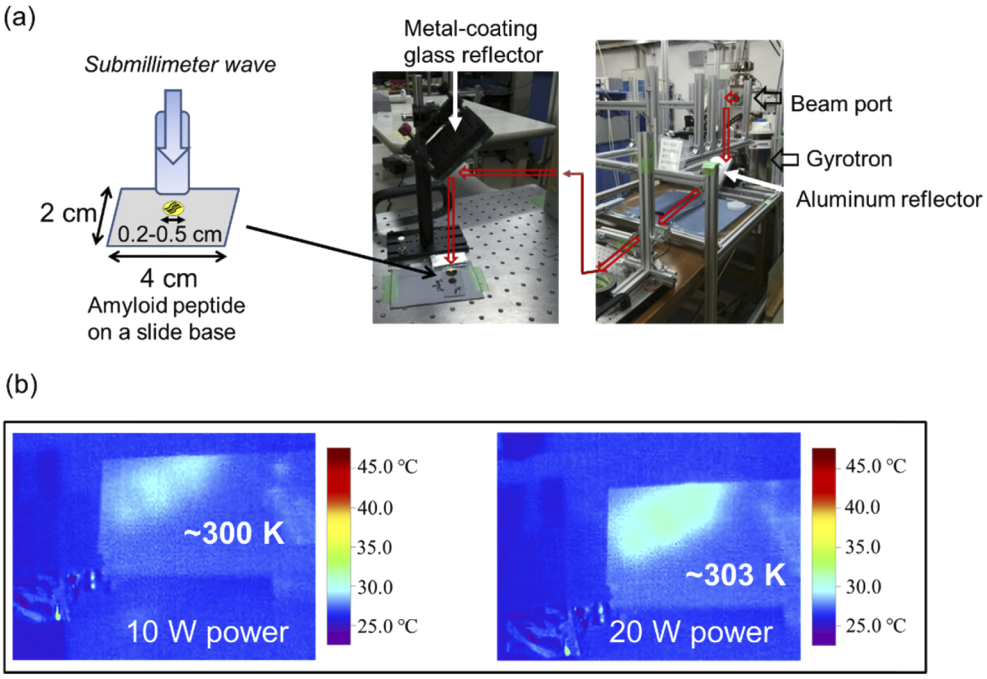

Fig. 1. Irradiation setup. (a) Beam line (red arrow) from the beam port to the sample. Amyloid peptide in aqueous solution was added on a slide base. The beam diameter was about 0.5-1 cm, which covered the whole surface of the sample. (b) Thermographic images on the sample surface during far-infrared radiations at 10 W (left) and 20 W (right).

When the GNNQQNY peptide was irradiated by the gyrotron at 20 W, scanning-electron microscopy (SEM) images clearly showed the solid, particle-like peptide was rearranged into an elongated needle-like structure (Fig. 2(a)-(b)). The thioflavin T (ThT) binding signal was substantially increased by the irradiation (Fig. 2(a)-(b), inserted panel). However, after 30-min incubations (room temperature and up to 318 K) without irradiation, the fluorescence value did not change (see Data File 1). In the SR-IRM spectra of the peptide (Fig. 2(c)), a strong peak at 1620 cm^{-1} and a weak peak at 1664 cm^{-1} were seen in the amide I ($\nu C=O$ stretching mode) region (Fig. 2(c), left). The former peak can be generally assigned to the amide I peak which contributes to the β-sheet stacking conformation [25,26]; the intensity of this peak was significantly increased after the irradiation (blue) compared to that before the irradiation (red). In the near-infrared range (Fig. 2(c), right), the O-H stretching mode was observed at 3270 cm^{-1}

Biomedical Optics EXPRESS

with a shoulder peak at 3410 cm^{-1}, and the latter peak intensity was clearly increased by the irradiation. Protein secondary structure analysis (Fig. 2(d)) showed that β-sheet content increased from about 50% to near 70% after irradiation. Further, α-helix, turn, and other conformations decreased after the 30-min irradiation (blue bar) compared to those in case of non-irradiation (red bar). In addition, the increased β-sheet content was not observed either at room temperature or 45 °C without irradiation (see Data File 2). These results demonstrate that the irradiation promoted the fibril formation at room temperature.

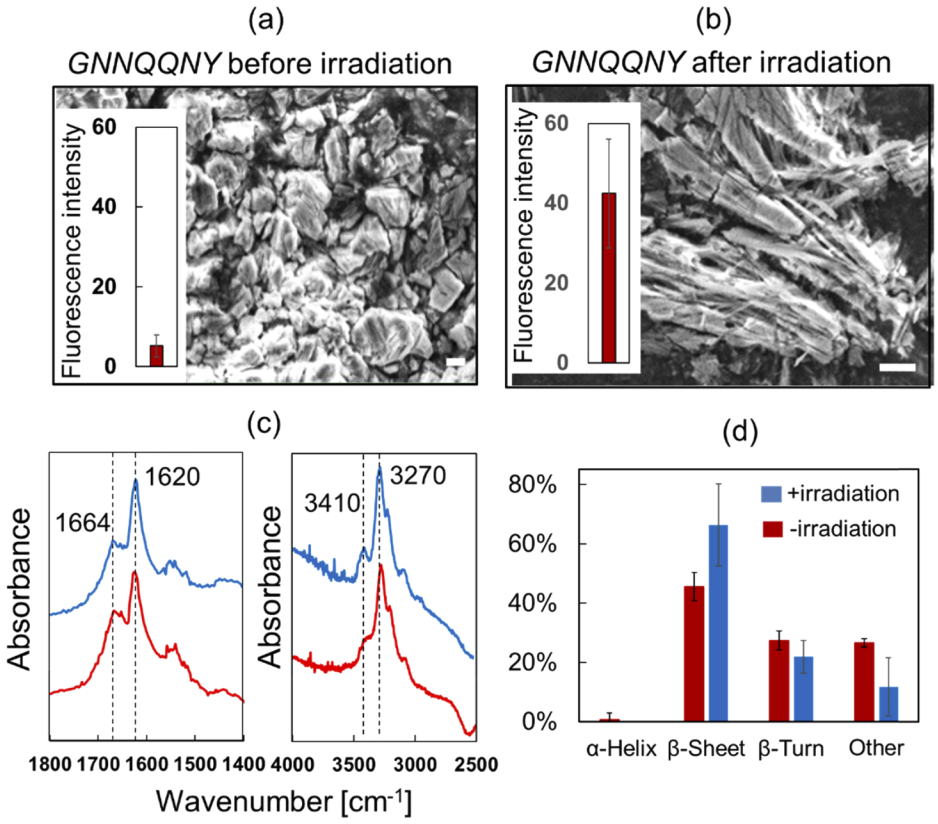

Fig. 2. Effect of irradiation on GNNQQNY. SEM images of the peptide before (a) and after irradiation at 20 W (b). Bar: 1 μm. Inserted panels: fluorescence intensities of thioflavin T. (c) Infrared spectra in the mid-infrared region (left) and near-infrared region (right). Red: without irradiation, blue: with irradiation. (d) Protein secondary structure analysis. Red: without irradiation, blue: with irradiation.

As seen in the SEM images of $A\beta_{1-40}$ (Fig. 3(a)-(b)), more aggregated solids were present after the 30-min irradiation (b) than before the irradiation (a). The ThT binding signal was obviously increased by the irradiation (Fig. 3(a)-(b), inserted panels). In the SR-IRM spectra of the non-irradiated sample (Fig. 3(c), red), the amide I band was observed at 1640 cm^{-1} with a shoulder peak at 1670 cm^{-1} (left panel) and a broad peak associated with O-H stretching vibration was observed at 3000-3500 cm^{-1} (right panel). After the irradiation (blue), the peak at 1640 cm^{-1} was sharpened and the shoulder peak was decreased, the intensity at amide II (N-H bending vibrational mode) around 1540 cm^{-1} was increased, and the O-H stretching vibrational peak at 3270 cm^{-1} was sharpened. Additionally, protein secondary structure analysis showed that β-sheet content was significantly increased from 50% to more than 60%, while turn and other conformations were decreased by the irradiation (Fig. 3(d)). In case of simple heating at 318 K

Biomedical Optics EXPRESS

(30 min incubation), the β-sheet, turn, and other conformations contents were about 40, 30, and 30%, respectively (see Data File 2 and Data File 3). These results indicate that aggregation of $A\beta_{1-40}$ was promoted, and the fibril content was increased by the far-infrared irradiation at room temperature. This observation is remarkable because the fibrillation of $A\beta_{1-40}$ proceeds slowly over several days under usual conditions at 37 °C.

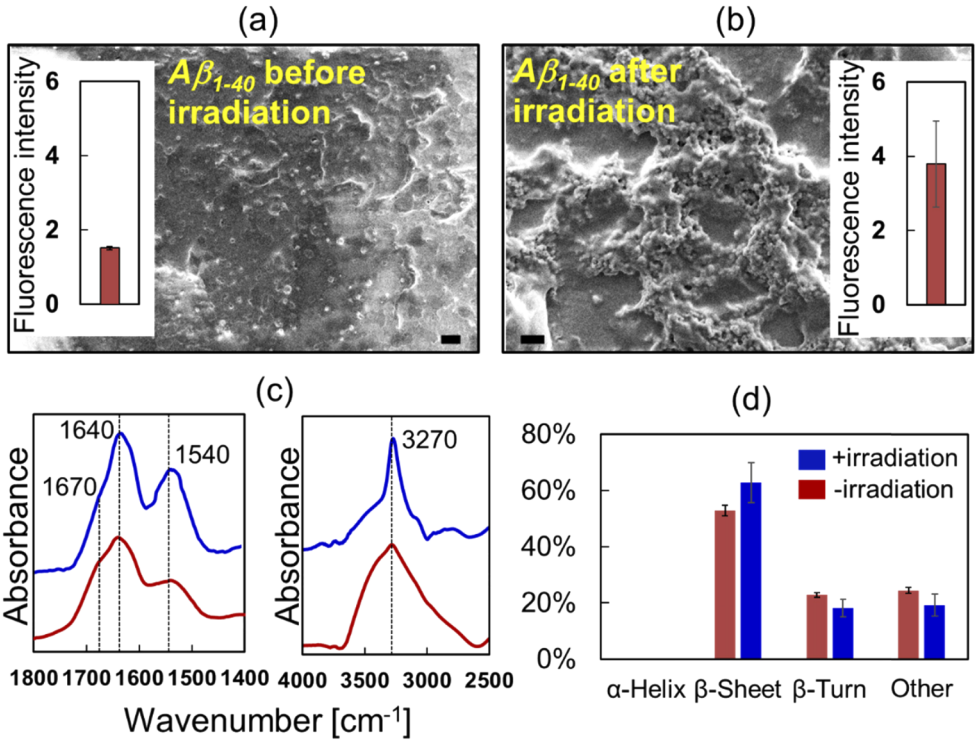

Fig. 3. Effect of irradiation on $A\beta_{1-40}$. SEM images before (a) and after (b) irradiation at room temperature. Bar: 1 μm. Inserted panels: fluorescent intensities of thioflavin T (see Data File 1). (c) Infrared spectra in the mid-infrared region (left) and near-infrared region (right). Red: without irradiation, blue: with irradiation. (d) Protein secondary structure analysis. Red: without irradiation, blue: with irradiation.

Next, we tested the effect of irradiation on SAA peptides. As shown in Fig. 4, the dry film of amyloidogenic SAA_{1-27} was observed as a black-colored aggregate on the metal base (Fig. 4(a)), whereas the non-amyloidogenic SAA_{51-80} was transparent and not aggregated (Fig. 4(b)). After far-infrared irradiation for 30 min (Fig. 4(c)), the morphology of the amyloidogenic SAA_{1-27} became darker and further aggregated compared to simple heating at 318 K without irradiation (upper left). The fluorescent ThT binding signal was substantially increased (white bars). On the other hand, neither the morphology nor the ThT value was changed in case of the non-amyloidogenic SAA_{51-80} (Fig. 4(d)). In addition, SAA_{1-27} increasingly aggregated in a time-dependent fashion during the 30 min irradiation (Fig. 4(e)). Thus, far-infrared irradiation promotes fibril aggregation of the amyloidogenic sequence, whereas nothing was found to stimulate the non-amyloidogenic one.

Finally, we investigated the effects of irradiation on DFNKF (Fig. 5). SEM observation revealed that the irradiation induced soft, cloth-like morphology after 10 minutes and the volume of the fibril increased after 1 hour of irradiation (Fig. 5(a)). The Congo-red stain (Fig. 5(b)) resulted in fibril-specific binding of the reagent (dotted circles) after the 10- and 30-min irradiation

Biomedical Optics EXPRESS

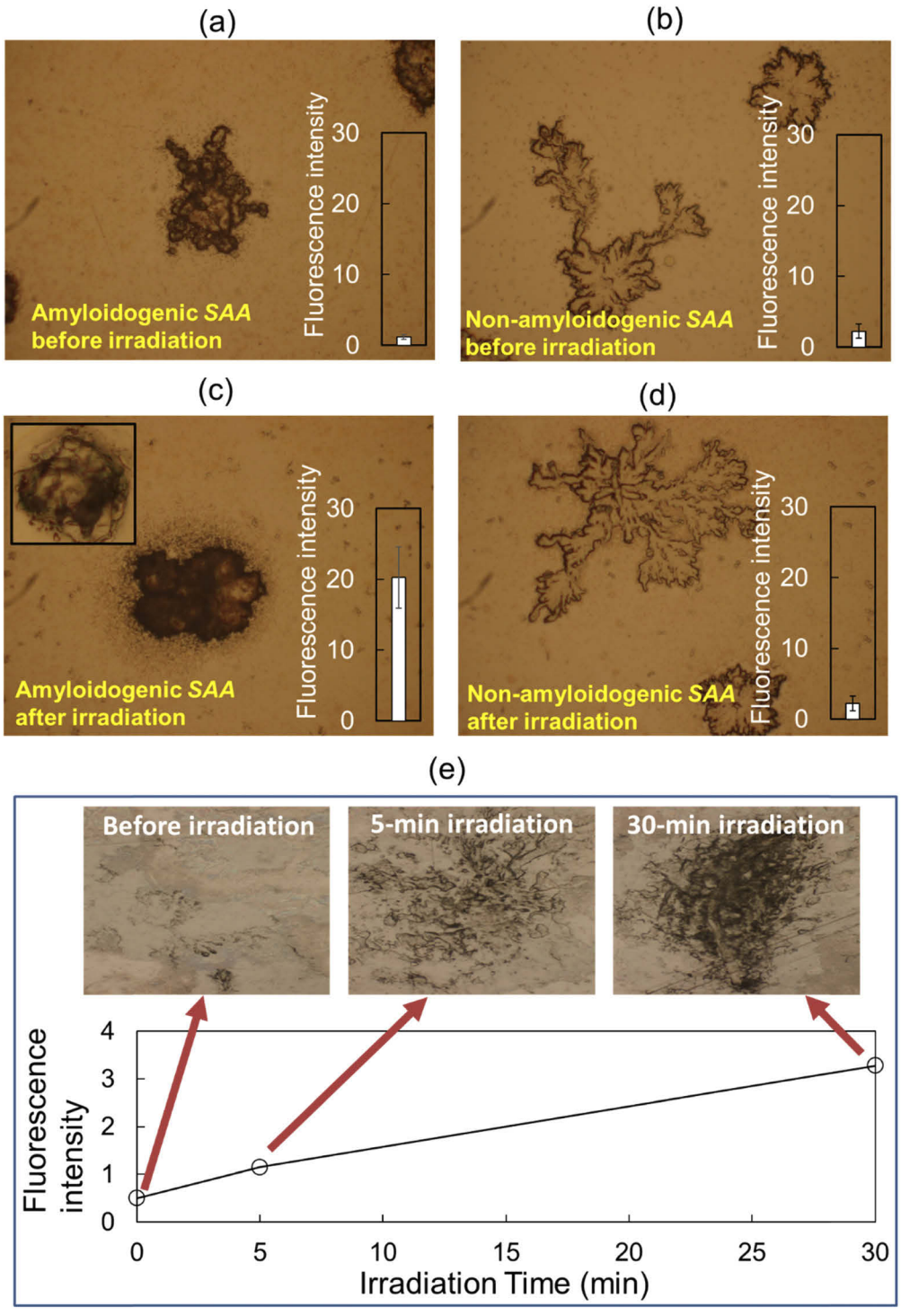

Fig. 4. Optical microscopy images and ThT binding signals of SAA (see Data File 1). (a) Amyloidogenic SAA_{1-27} before irradiation. (b) Non-amyloidogenic SAA_{51-80} before irradiation. (c) Amyloidogenic SAA_{1-27} after irradiation and heating at 318 K (upper left) for 30 min. (d) Non-amyloidogenic SAA_{51-80} after irradiation for 30 min. (e) Irradiation time dependency. The radiation beam was focused on to the sample using a Teflon lens, and the irradiation power was set to 150 mJ/cm^2. Horizontal scale of the image: 500 μm.

Biomedical Optics EXPRESS

compared to the sample before irradiation and the non-irradiated samples. As shown in Fig. 5(c), there are two bands in the amide I region (1600-1700cm^{-1}) of the non-irradiated peptide: one is a peak at 1630 cm^{-1} that contributes to the amide C = O stretching mode in the main chain of the fibril structure, and another is at 1670 cm^{-1} which corresponds to the other amide bonds including side chains [26]. In the case of simple incubation without irradiation for 30 min at 37 °C, those band intensities were approximately equal to those of the peptide before incubation (0 min), and the former peak intensity was increased over 1 day compared to the latter peak. On the other hand, in case of irradiation (Fig. 5(d)), the peak intensity at 1630 cm^{-1} was increased by 10 to 30 min irradiation. Therefore, the far-infrared irradiation promoted fibril formation in the DFNKF peptide at room temperature compared to spontaneous self-association at 310 K.

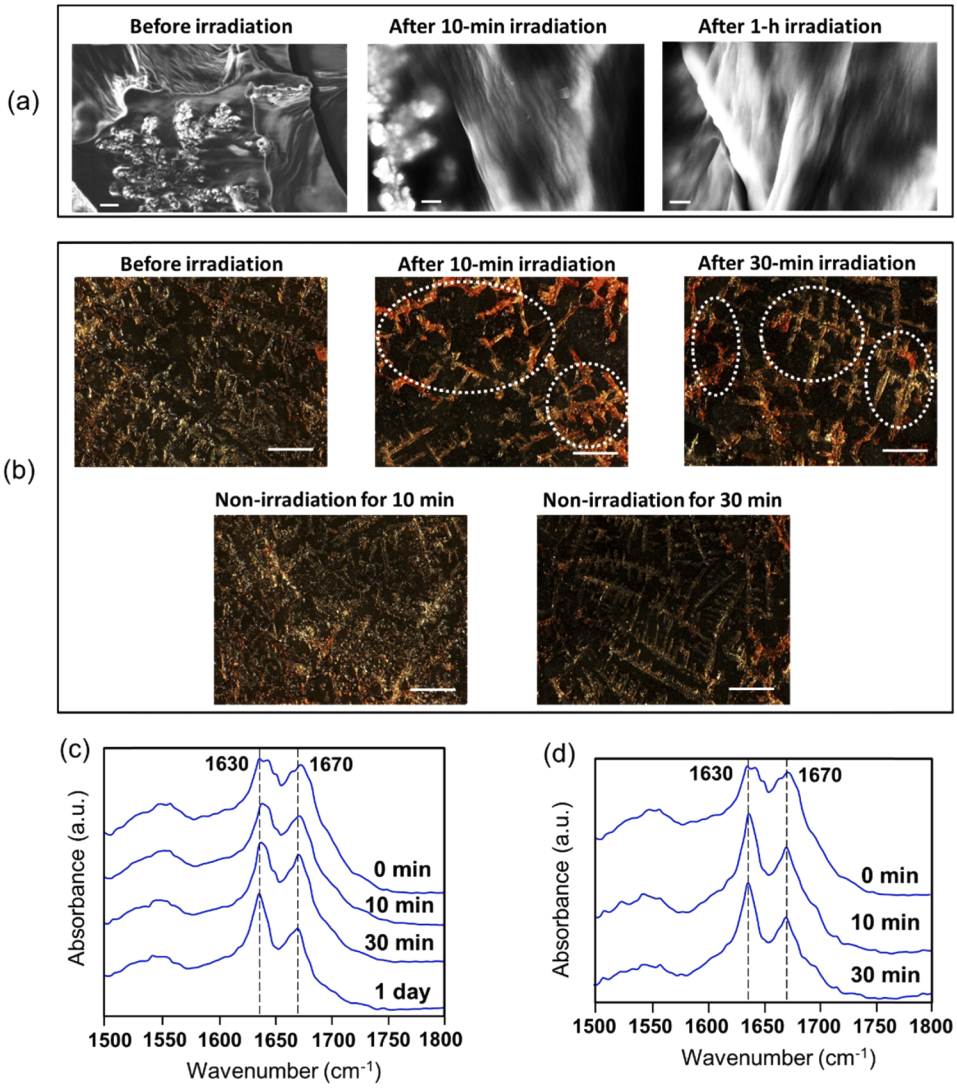

Fig. 5. Effect of irradiation on DFNKF. (a) SEM images before and after the irradiation. Bar: 1 μm. (b) Congo-red stain. Bar: 40 μm. (c) Infrared spectra at amide I region without irradiation. (d) Infrared spectra at amide I region with irradiation.

Biomedical Optics EXPRESS

4. Discussion

This study demonstrated that amyloidogenic peptides form fibrous aggregates at near room temperature after far-infrared irradiation whereas non-amyloidogenic peptides were not affected by the irradiation. The promotion of amyloid self-assembly by the radiation was much more pronounced than by simple heating. In several previous studies, it was reported that amyloid aggregation can be stimulated by microwave irradiation [27,28]. However, those systems typically require high temperatures (50 to 100 °C) to operate the irradiation system. Our system, which uses the gyrotron, requires no external heating and negligibly heats the target samples. Our results indicate that irradiation experiments can be performed under mild conditions to induce amyloid fibrillation. Several studies have investigated the non-thermal effects by using far-infrared radiation on the biological materials [29,30], and a recent paper demonstrated that double-stranded DNA can be disassembled *kinetically* (not thermodynamically) by THz picosecond pulses [30]. The authors demonstrated clear differences in the radiation effect on biomolecules induced by microwave and THz pulse beam, and the study recommends the proper use of far-infrared radiation techniques depending on the target material.

In our prior work using an infrared free electron laser, we found that the fibrous conformation of amyloidogenic peptides was dissociated by the terahertz free electron laser (FEL) and amide-I specific irradiation, in contrast to the effect achieved by the submillimeter wave radiation from the gyrotron in this study [31,32]. In the case of the FEL, the vibrational excitation of the amide bonds induced by successive irradiation with picosecond pulses can dissociate the hydrogen bonds in the β-sheet stacking structure [33]. In this work, however, the pulse duration is on the scale of milliseconds and the oscillation wavelengths are several hundred micrometers. Regarding the mechanism, Yamazaki et al. indicated that far-infrared irradiation promotes the polymerization of actin filaments in cell, suggesting that the submillimeter wave corresponds to intermolecular motions and induces conformational changes in the protein [14]. Thus, far-infrared radiation can stimulate the self-association of peptides and amyloid fibrils can be induced to form aggregates by the sub-terahertz wave from a gyrotron.

Future work will determine the applicability of our findings in the biomedical and materials fields. Our system may be employed for the rapid screening of inhibitors for amyloid fibrillation. The sub-terahertz radiation system used in this work can shorten the fibril elongation time to ~30 min, whereas the conventional process usually takes several hours to days [34]. This advantage, combined with computational techniques, will allow us to study amyloid fibril formation [8,35]. The system will also contribute to the processing of fibrous biomaterials. Certain electric and magnetic fields can change the structures of proteins and peptides, and physical engineering techniques using electromagnetic wave radiation may lead to structural control and functional design of biomaterials [36]. The submillimeter wave radiation system has the potential to produce an artificial fibril structure of amyloid peptides on a metal base without specific chemical modifications [37]. However, further investigation of the elongation mechanism of the fibrous conformation of amyloid peptides is required. The infrared FEL can dissociate the fibril structure of the amyloid peptide by cleaving the hydrogen bonds in the β-sheet stacked conformations [38], and the use of the infrared FEL will allow us to investigate whether the aggregation and dissociation are reversible or not. This theme regarding the fibril formation mechanism should be a next subject of our research group.

5. Conclusion

We irradiated four kinds of amyloidogenic peptides (GNNQQNY, $A\beta_{1-40}$, SAA_{1-27}, and DFNKF) on a slide base at room temperature using a gyrotron that emits 720 μm waves at 420 GHz. A Thioflavin T assay, microscopy observation, and Congo-red staining showed that all amyloidogenic peptides were induced to form fibril structures while a non-amyloidogenic SAA_{51-80} fragment

Biomedical Optics EXPRESS

was not influenced by the radiation. SR-IRM analysis showed that the β-sheet conformations in GNNQQNY, $A\beta_{1-40}$, and DFNKF were increased by the irradiation. In this system, the temperature of the sample surface increased by less than 5 K as observed by a thermography camera. This study showed for the first time that a submillimeter wave promotes amyloidogenic aggregation with little thermal effect *in vitro*. We expect that the far-infrared radiation system suggested herein will be used in various biological and material fields associated with amyloid fibrils.

Funding

Private University Research Branding Project organized (MEXT) for Water Frontier Science & Technology Research Center of Tokyo University of Science; Open Advanced Research Facilities Initiative and Photon Beam Platform Project of the Ministry of Education, Culture, Sports, Science and Technology, Japan; Japan Society for the Promotion of Science (JP20K12483).

Acknowledgements

This work was supported in part by a collaborative research with SR Center of Ritsumeikan University (subject number: S18006 in 2018) and the collaborative research project of the Research Center for Development of the Far-Infrared Region, University of Fukui, in the fiscal years 2018 and 2019 (subject number: H30FIRDM015C and R01FIRDM020A, respectively).

Disclosures

The authors declare that there are no conflicts of interest related to this article.

References

1. S. L. Pedersen, A. P. Tofteng, L. Malik, and K. J. Jensen, "Microwave heating in solid-phase peptide synthesis," Chem. Soc. Rev. **41**(5), 1826–1844 (2012).
2. S. Horikoshi and N. Serpone, "Microwave Flow Chemistry as a Methodology in Organic Syntheses, Enzymatic Reactions, and Nanoparticle Syntheses," Chem. Rec. **19**(1), 118–139 (2019).
3. G. J. Wilmink, B. D. Rivest, C. C. Roth, B. L. Ibey, J. A. Payne, L. X. Cundin, J. E. Grundt, X. Peralta, D. G. Mixon, and W. P. Roach, "In vitro investigation of the biological effects associated with human dermal fibroblasts exposed to 2.52 THz radiation," Lasers Surg. Med. **43**(2), 152–163 (2011).
4. F. Vatansever and M. R. Hamblin, "Far infrared radiation (FIR): its biological effects and medical applications," Photonics Lasers Med. **1**(4), 255–266 (2012).
5. I. N. Chiang, Y. S. Pu, C. Y. Huang, and T. H. Young, "Far infrared radiation promotes rabbit renal proximal tubule cell proliferation and functional characteristics, and protects against cisplatin-induced nephrotoxicity," PLoS One **12**(7), e0180872 (2017).
6. P. Tewari, J. Garritano, N. Bajwa, S. Sung, H. Huang, D. Wang, W. Grundfest, D. B. Ennis, D. Ruan, E. Brown, E. Dutson, M. C. Fishbein, and Z. Taylor, "Methods for registering and calibrating in vivo terahertz images of cutaneous burn wounds," Biomed. Opt. Express **10**(1), 322–337 (2019).
7. M. D. Benson, J. N. Buxbaum, D. S. Eisenberg, G. Merlini, M. J. M. Saraiva, Y. Sekijima, J. D. Sipe, and P. Westermark, "Amyloid nomenclature 2018: recommendations by the International Society of Amyloidosis (ISA) nomenclature committee," Amyloid **25**(4), 215–219 (2018).
8. P. Nguyen and P. Derreumaux, "Understanding amyloid fibril nucleation and aβ oligomer/drug interactions from computer simulations," Acc. Chem. Res. **47**(2), 603–611 (2014).
9. D. M. Fowler, A. V. Koulov, W. E. Balch, and J. W. Kelly, "Functional amyloid – from bacteria to humans," Trends Biochem. Sci. **32**(5), 217–224 (2007).
10. C. Li, R. Qin, R. Liu, S. Miao, and P. Yang, "Functional amyloid materials at surfaces/interfaces," Biomater. Sci. **6**(3), 462–472 (2018).
11. S. Das, R. S. Jacob, K. Patel, N. Singh, and S. K. Maji, "Amyloid Fibrils: Versatile Biomaterials for Cell Adhesion and Tissue Engineering Applications," Biomacromolecules **19**(6), 1826–1839 (2018).
12. S. T. Han, R. G. Griffin, K. N. Hu, C. G. Joo, C. D. Joye, I. Mastovsky, M.A Shapiro, J. R. Sirigiri, R. J. Temkin, A. C. Torrezan, and P.P Woskov, "Continuous-wave Submillimeter-wave Gyrotrons," Proc. SPIE **6373**, 63730C (2006).
13. M. Pilossof and M. Einat, "Note: A 95 GHz mid-power gyrotron for medical applications measurements," Rev. Sci. Instrum. **86**(1), 016113 (2015).
14. S. Yamazaki, M. Harata, T. Idehara, K. Konagaya, G. Yokoyama, H. Hoshina, and Y. Ogawa, "Actin polymerization is activated by terahertz irradiation," Sci. Rep. **8**(1), 9990 (2018).

Biomedical Optics EXPRESS

15. A. M. Portillo, A. V. Krasnoslobodtsev, and Y. L. Lyubchenko, "Effect of electrostatics on aggregation of prion protein Sup35 peptide," J. Phys.: Condens. Matter **24**(16), 164205 (2012).
16. J. R. Lewandowski, P. C. van der Wel, M. Rigney, N. Grigorieff, and R. G. Griffin, "Structural complexity of a composite amyloid fibril," J. Am. Chem. Soc. **133**(37), 14686–14698 (2011).
17. W. Qiang, W. M. Yau, J. X. Lu, J. Collinge, and R. Tycko, "Structural variation in amyloid-β fibrils from Alzheimer's disease clinical subtypes," Nature **541**(7636), 217–221 (2017).
18. L. Vugmeyster, M. A. Clark, I. B. Falconer, D. Ostrovsky, D. Gantz, W. Qiang, and G. L. Hoatson, "Flexibility and Solvation of Amyloid-β Hydrophobic Core," J. Biol. Chem. **291**(35), 18484–18495 (2016).
19. G. Nys, G. Cobraiville, A. C. Servais, M. G. Malaise, D. de Seny, and M. Fillet, "Targeted proteomics reveals serum amyloid A variants and alarmins S100A8-S100A9 as key plasma biomarkers of rheumatoid arthritis," Talanta **204**, 507–517 (2019).
20. S. Claus, K. Meinhardt, T. Aumüller, I. Puscalau-Girtu, J. Linder, C. Haupt, P. Walther, T. Syrovets, T. Simmet, and M. Fändrich, "Cellular mechanism of fibril formation from serum amyloid A1 protein," EMBO Rep. **18**(8), 1352–1366 (2017).
21. F. Rigoldi, P. Metrangolo, A. Redaelli, and A. Gautieri, "Nanostructure and stability of calcitonin amyloids," J. Biol. Chem. **292**(18), 7348–7357 (2017).
22. N. Haspel, D. Zanuy, B. Ma, H. Wolfson, and R. Nussinov, "A comparative study of amyloid fibril formation by residues 15-19 of the human calcitonin hormone: a single beta-sheet model with a small hydrophobic core," J. Mol. Biol. **345**(5), 1213–1227 (2005).
23. T. Idehara and S. P. Sabchevski, "Gyrotrons for High-Power Terahertz Science and Technology at FIR UF," J. Infrared, Millimeter, Terahertz Waves **38**(1), 62–86 (2017).
24. T. Yaji, Y. Yamamoto, T. Ohta, and S. Kimura, "A new beamline for infrared microscopy in the SR center of Ritsumeikan University," Infrared Phys. Technol. **51**(5), 397–399 (2008).
25. T. Kawasaki, J. Fujioka, T. Imai, and K. Tsukiyama, "Effect of Mid-infrared Free-Electron Laser Irradiation on Refolding of Amyloid-Like Fibrils of Lysozyme into Native Form," Protein J. **31**(8), 710–716 (2012).
26. M. Reches, Y. Porat, and E. Gazit, "Amyloid fibril formation by pentapeptide and tetrapeptide fragments of human calcitonin," J. Biol. Chem. **277**(38), 35475–35480 (2002).
27. D. I. de Pomerai, B. Smith, A. Dawe, K. North, T. Smith, D. B. Archer, I. R. Duce, D. Jones, and E. P. Candido, "Microwave radiation can alter protein conformation without bulk heating," FEBS Lett. **543**(1-3), 93–97 (2003).
28. C. A. Hettiarachchi, L. D. Melton, J. A. Gerrard, and S. M. Loveday, "Formation of β-lactoglobulin nanofibrils by microwave heating gives a peptide composition different from conventional heating," Biomacromolecules **13**(9), 2868–2880 (2012).
29. A. Peinnequin, A. Piriou, J. Mathieu, V. Dabouis, C. Sebbah, R. Malabiau, and J. C. Debouzy, "Non-thermal effects of continuous 2.45 GHz microwaves on Fas-induced apoptosis in human Jurkat T-cell line," Bioelectrochemistry **51**(2), 157–161 (2000).
30. A. A. Greschner, X. Ropagnol, M. Kort, N. Zuberi, J. Perreault, L. Razzari, T. Ozaki, and M. A. Gauthier, "Room-Temperature and Selective Triggering of Supramolecular DNA Assembly/Disassembly by Nonionizing Radiation," J. Am. Chem. Soc. **141**(8), 3456–3469 (2019).
31. T. Kawasaki, K. Tsukiyama, and A. Irizawa, "Dissolution of a fibrous peptide by terahertz free electron laser," Sci. Rep. **9**(1), 10636 (2019).
32. T. Kawasaki, T. Yaji, T. Ohta, K. Tsukiyama, and K. Nakamura, "Dissociation of β-Sheet Stacking of Amyloid β Fibrils by Irradiation of Intense, Short-Pulsed Mid-infrared Laser," Cell. Mol. Neurobiol. **38**(5), 1039–1049 (2018).
33. V. H. Man, P. Derreumaux, M. S. Li, C. Roland, C. Sagui, and P. H. Nguyen, "Picosecond dissociation of amyloid fibrils with infrared laser: A nonequilibrium simulation study," J. Chem. Phys. **143**(15), 155101 (2015).
34. M. Raju, P. Santhoshkumar, and K. K. Sharma, "Cell-penetrating Chaperone Peptide Prevents Protein Aggregation And Protects Against Cell Apoptosis," Adv. Biosyst. **2**(1), 1700095 (2018).
35. S. Sen, L. Vuković, and P. Král, "Computational screening of nanoparticles coupling to Aβ40 peptides and fibrils," Sci. Rep. **9**(1), 17804 (2019).
36. G. Pandey, J. Saikia, S. Sasidharan, D. C. Joshi, S. Thota, H. B. Nemade, N. Chaudhary, and V. Ramakrishnan, "Modulation of Peptide Based Nano-Assemblies with Electric and Magnetic Fields," Sci. Rep. **7**(1), 2726 (2017).
37. S. H. Ku and C. B. Park, "Highly accelerated self-assembly and fibrillation of prion peptides on solid surfaces," Langmuir **24**(24), 13822–13827 (2008).
38. T. Kawasaki, V. H. Man, Y. Sugimoto, N. Sugiyama, H. Yamamoto, K. Tsukiyama, J. Wang, P. Derreumaux, and P. H. Nguyen, "Infrared Laser-Induced Amyloid Fibril Dissociation: A Joint Experimental/Theoretical Study on the GNNQQNY Peptide," J. Phys. Chem. B **124**(29), 6266–6277 (2020).